Lattice Boltzmann Model for the Charney-Hasegawa-Mima equation

M. Held, A. Kendl

Institue for Ion Physics and Applied Physics, University of Innsbruck,

Technikerstr. 25, A-6020 Innsbruck, Austria

Introduction

The Charney-Hasegawa-Mima (CHM) equation serves as a basic prototypical two-dimensional one-field model for electrostatic drift wave turbulence in magnetised plasmas with cold ions and isothermal adiabatic electrons [1]

$$\left(1-\nabla^2\right)\frac{\partial\delta\phi}{\partial t}+\frac{\partial\delta\phi}{\partial y}-\left\{\delta\phi,\nabla^2\delta\phi\right\}=0 \tag{1}$$

The equation is normalized according to $\boldsymbol{x}\leftarrow\boldsymbol{x}/\rho_s$ and $t\leftarrow\kappa_n\omega_{ci}t$ for the length and time scales, and $\delta\phi\leftarrow\kappa_n^{-1}(e\phi/T_e)$ for the electrostatic potential ϕ. Here $\kappa_n=\rho_s/L_n$ is the drift ratio between the drift scale $\rho_s=\sqrt{m_iT_e}/eB$ (corresponding to a gyro radius of ions of mass m_i at electron temperature T_e) and the gradient length $L_n=|\partial_x\ln n_0(x)|^{-1}$ of the static background density $n_0(x)$. The sound speed enters as $c_s=\sqrt{T_e/m_i}$, and the gyro frequency as $\omega_{ci}=c_s/\rho_s$. The CHM equation can be obtained from the continuity and momentum equations for a cold uniformally magnetised ion fluid ($T_i\ll T_e$) with adiabatic electron response and a negative background density gradient in x-direction, $n_i=n_e=n_0(x)\exp[e\phi/kT_e]$. The normalized ion continuity and momentum equations can be expressed in terms of the potential instead of density as [1]

$$\kappa_n\frac{d}{dt}\delta\phi+\boldsymbol{\nabla}\cdot\boldsymbol{u} = \kappa_n\,\boldsymbol{u}\cdot\boldsymbol{\nabla}x \tag{2}$$

$$\kappa_n\frac{d}{dt}\boldsymbol{u}+\boldsymbol{e}_z\times\boldsymbol{u} = -\boldsymbol{\nabla}\delta\phi \tag{3}$$

where $d/dt=\partial_t+\boldsymbol{u}\cdot\boldsymbol{\nabla}$ is the advective derivative. The implemented lattice Boltzmann model (LBM) makes use of the last two equations, since these equations resemble CHM dynamics under drift ordering ($\kappa_n\ll 1$).

Lattice Boltzmann model

The most important ingredients of the LBM are specified as follows

1. Lattice geometry

   The implementation of an D2Q9 lattice (2 dimensions, 9 lattice velocities $\boldsymbol{\xi}_i$) fixes the lattice speed of sound $c_L=(1/\sqrt{3})(\delta x/\delta t)=\sqrt{\theta}(\delta x/\delta t)$ and the weights $w_i=\{\frac{4}{9},\frac{1}{9},\frac{1}{9},\frac{1}{9},\frac{1}{9},\frac{1}{36},\frac{1}{36},\frac{1}{36},\frac{1}{36}\}$ [2].

2. Discretization technique and collision operator

   The Collision step is approximated by the trapezoid rule, which turns the lattice Boltzmann equation into an implicit relation. Hence an transformation from $f_i \leftarrow \bar{f}_i$ is applied to obtain a similar explicit scheme for $\bar{f}_i$, which however leads to an implicit relations for the velocity moments over the distribution function f_i [5]. This implicitness is bypasses by a well founded incompressible approximation for the potential and velocity shifts which avoids an implementation of e.g. Newton's method. The relaxation of the distribution function to local Maxwellian equlibrium is untertaken by the Bathnagar-Gross-Krook (BGK) operator with a single relaxation time τ^*. Hence the lattice Boltzmann equation is split up into the collision step

$$\bar{f}_i^*(\boldsymbol{x},t) = \bar{f}_i(\boldsymbol{x},t) - \frac{2}{2\tau^*+1}\left(\bar{f}_i(\boldsymbol{x},t) - f_i^{eq}(\boldsymbol{x},t)\right) + \frac{2\tau^*\delta t}{2\tau^*+1}F_i(\boldsymbol{x},t); \tag{4}$$

   and the streaming step

$$\bar{f}_i(\boldsymbol{x}+\boldsymbol{\xi}_i\delta t, t+\delta t) = \bar{f}_i^*(\boldsymbol{x},t); \tag{5}$$

   with the approximated potential and velocity shifts

$$\phi \leftarrow \frac{\bar{\phi}}{1-\frac{\delta t}{2}\frac{1}{L_n}\boldsymbol{u}\cdot\boldsymbol{e}_x} \tag{6}$$

$$\boldsymbol{u} \leftarrow \frac{\bar{\boldsymbol{u}} - \frac{\delta t}{2}\omega_{ci}(\boldsymbol{e}_z\times\bar{\boldsymbol{u}})}{1+\left(\frac{\delta t}{2}\omega_{ci}\right)^2}\left(1-\frac{\delta t}{2}\frac{1}{L_n}\boldsymbol{u}\cdot\boldsymbol{e}_x\right) \tag{7}$$

3. Equilibrium distribution function (EDF)

   The barotropic equation of state $P = \phi^2/(2\kappa_n^2)$ of the macroscopic equations together with the lattice geometry determines the EDF to [3]

$$\begin{aligned} f_0^{eq} &= w_0\phi\left[\frac{9}{4} - \frac{5}{4}\frac{P(\phi)}{\phi\theta} - \frac{\boldsymbol{u}^2}{2\theta}\right] \\ f_i^{eq} &= w_i\phi\left[\frac{P(\phi)}{\phi\theta} + \frac{\boldsymbol{\xi}_i\cdot\boldsymbol{u}}{\theta} + \frac{(\boldsymbol{\xi}_i\cdot\boldsymbol{u})^2}{2\theta^2} - \frac{\boldsymbol{u}^2}{2\theta}\right]. \end{aligned} \tag{8}$$

4. Forcing function (FF) with source and force terms

   An augmented FF [4] is derived to reproduce the dynamics of the nonsteady and non-uniform density gradient source term

$$s = \kappa_n\boldsymbol{u}\cdot\boldsymbol{e}_x, \tag{9}$$

   and Lorentz force term

$$\boldsymbol{a} = \frac{1}{\kappa_n}(\boldsymbol{u}\times\boldsymbol{e}_z) + \boldsymbol{u}s, \tag{10}$$

which contains a cross product and a correction, which cancels a spurious term in the momentum equation. The latter two equations enter the adapted FF in its present form

$$F_i = w_i \phi \left\{ \left[1 + \left(\theta - \frac{dP}{d\phi} \right) \left(\frac{4+g_i}{4\theta} - \frac{\boldsymbol{\xi}_i^2}{2\theta^2} \right) \right] s + \left[\frac{(\boldsymbol{\xi}_i - \boldsymbol{u})}{\theta} + \frac{(\boldsymbol{\xi}_i \cdot \boldsymbol{u})\boldsymbol{\xi}_i}{\theta^2} \right] \cdot \boldsymbol{a} \right\} \quad (11)$$

with $g_i = \{1, -2, -2, -2, -2, 4, 4, 4, 4\}$.

5. Boundary conditions

   For stability reasons, free-slip boundary conditions are chosen on the east and west boundaries (in "radial" direction in terms of drift wave terminology), whereas the north and south boundaries (in "poloidal" direction) are treated periodically [2]. The rigid walls on east and west are set on the outermost lattice nodes, which corresponds to an on-site reflection of the perpendicular components of $\bar{f}$. On east the distribution function is flipped according to $\bar{f}_3 \rightarrow \bar{f}_1$, $\bar{f}_6 \rightarrow \bar{f}_5$, $\bar{f}_7 \rightarrow \bar{f}_8$, and vice versa for the west boundary.

Numerical test results

The proposed LB model (first row of the figures) is cross-verified with a conventional finite difference scheme (second row) which directly solves the CHM eq., including an artificial hyperviscocity. This FD scheme uses a 3rd order multi-step method for time integration, an Arakawa discretization of the Poisson brackets, and an FFT Poisson solver [6]. For all following computations the drift parameter is set to $\kappa_n = 0.05$, the normalized box size is fixed to $L_0 = 64$, and the LB viscosity to $\nu = 0.0002$. Furthermore a resolution of $N_x = N_y = 2048$ is chosen, which fullfills the stability criterion $(\delta t / \delta x^2) \approx 1$ for these parameters. The three test cases dispersive spreading of a monopole (first column of Fig. 1), stable drift modon propagation (second column of Fig. 1) and decaying turbulence (third column of Fig. 1) reflect the expected drift wave turbulence behaviour, except for the drift modon case. Here the incompressible approximation in the velocity shifts (eq. (6) and (7)) causes to break the stability of the drift modon by a slight shear. This deviation disappears for highly incompressible flows with drift parameters of $\kappa_n \leq 0.001$. The computational performance of our present LBM implementation lags a little behind the employed conventional method. Nevertheless the LBM is preferably applicable for highly resolved (in time and space) numerical investigations once its full potential of parallelization is exploited, since the deviations would disappear in this limit.

Acknowledgement

This work was partly supported by the Austrian Science Fund (FWF) Y398; by the Austrian Ministry of Science BMWF as part of the UniInfrastrukturprogramm of the Research Platform

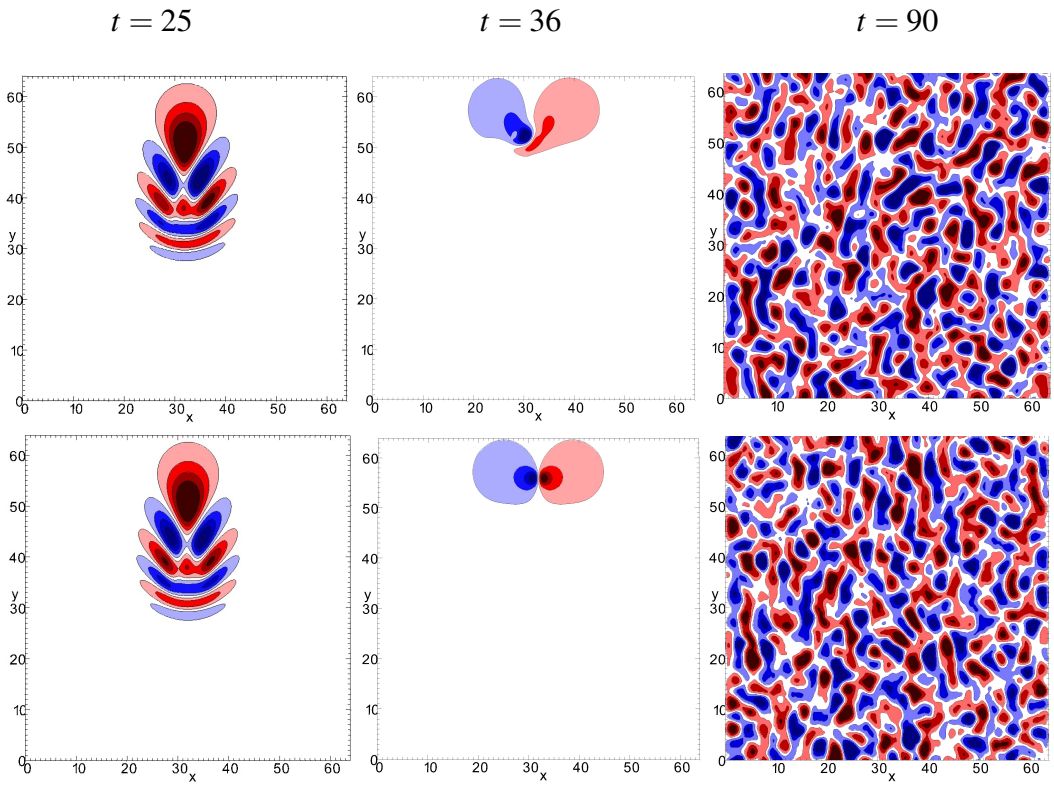

Figure 1: The first column shows the dispersive spreading of an initial monopole with small amplitude. The second column reflects the distortion of a stable drift modon by a small shear. The third column presents the advanced state of the turbulent potential field. The tendency to large scale zonally extended structures is visible.

Scientific Computing at the University of Innsbruck; and by the European Commission under the Contract of Association between EURATOM and ÖAW carried out within the framework of the European Fusion Development Agreement (EFDA). The views and opinions expressed herein do not necessarily reflect those of the European Commission.

References

[1] W. Horton and A. Hasegawa, Chaos 4, 227 (1994).

[2] S. Succi, *The Lattice Boltzmann Equation for Fluid Dynamics and Beyond.* Oxford University Press, 2001.

[3] P.J. Dellar, Phys. Rev. E, 65, 036309 (2002).

[4] Y. Cheng, J. Li International Journal for Numerical Methods in Fluids 6, 629 (2008).

[5] P.J. Dellar, Computers & Mathematics with Applications 65, 129 (2013)

[6] V. Naulin and A.H. Nielsen, SIAM J. Sci. Comput. 25, 104 (2003).